

# Floquet Topological Insulator in Semiconductor Quantum Wells

Netanel H. Lindner<sup>1</sup>, Gil Refael<sup>1,2</sup>, Victor Galitski<sup>3,4</sup>

1) *Institute of Quantum Information, California Institute of Technology, Pasadena, CA 91125, USA.*

2) *Department of Physics, California Institute of Technology, Pasadena, CA 91125, USA.*

3) *Condensed Matter Theory Center, Department of Physics,  
University of Maryland, College Park, Maryland 20742, USA. and*

4) *Joint Quantum Institute, Department of Physics,  
University of Maryland, College Park, Maryland 20742, USA*

Topological phase transitions between a conventional insulator and a state of matter with topological properties have been proposed and observed in mercury telluride - cadmium telluride quantum wells. We show that a topological state can be induced in such a device, initially in the trivial phase, by irradiation with microwave frequencies, without closing the gap and crossing the phase transition. We show that the quasi-energy spectrum exhibits a single pair of helical edge states. The velocity of the edge states can be tuned by adjusting the intensity of the microwave radiation. We discuss the necessary experimental parameters for our proposal. This proposal provides an example and a proof of principle of a new non-equilibrium topological state, Floquet topological insulator, introduced in this paper.

Topological phases of matter have captured our imagination over the past few years, with tantalizing properties such as robust edge modes and exotic non-Abelian excitations [1, 2], and potential applications ranging from semiconductor spintronics [3] to topological quantum computation [4]. The discovery of topological insulators in solid-state devices such as HgTe/CdTe quantum wells [5, 6], and in materials such as Bi<sub>2</sub>Te<sub>3</sub>, Bi<sub>2</sub>Sn<sub>3</sub> [7–9] brings us closer to employing the unique properties of topological phases in technological applications.

Despite this success, however, the choice of materials that exhibit these unique topological properties remains rather scarce. In most cases we have to rely on serendipity in looking for topological materials in solid-state structures and our means to engineer Hamiltonians there are very limited. Therefore, to develop new methods to achieve and control topological structures at will would be of great importance.

Our work demonstrates that such new methods are indeed possible in non-equilibrium, where external time-dependent perturbations represent a rich and versatile resource that can be utilized to achieve topological spectra in systems that are topologically trivial in equilibrium. In particular, we show that periodic-in-time perturbations may give rise to new differential operators with topological insulator spectra, dubbed Floquet topological insulators (FTI), that exhibit chiral edge currents in non-equilibrium and possess other hallmark phenomena associated with topological phases. These ideas, put together with the highly developed technology for controlling low-frequency electromagnetic modes, can enable devices in which fast switching of edge state transport is possible. Moreover, the spectral properties of the edge states, i.e., their velocity, and the bandgap of the bulk insulator, can be easily controlled. On a less applied perspective, the fast formation of the Floquet topological insulators in response to the external field opens a path to study quench

dynamics of topological states in solid-state devices.

The Floquet topological insulators discussed here share many features discussed in some previous works: The idea of achieving topological states in a periodic Hamiltonian was also explored from the perspective of quantum walks in Ref. 10. Also, a similar philosophy led to proposals for the realization of topological phases in cold-atom systems: a quantum Hall state using a stroboscopic quadrupole field [11] and a topological insulator state using a Ramann-scattering induced spin-orbit coupling [12]. Also, Ref. [13] proposed to use a circularly-polarized light field to induce a Hall current in graphene. Another useful analogy for our work is the formation of zero-resistance state in Hall bars at low magnetic fields using RF radiation [14–17]. In our case, it is not the resistance of the bulk that vanishes, but rather the resistance of the edges, which becomes finite and universal upon application of the light field. As we were finalizing our draft, we also became aware of Ref. 18, which proposed to use a periodic modulation in the form of a circularly polarized light to change the Chern number in the Haldane model [19].

## DEFINITION OF A FLOQUET TOPOLOGICAL INSULATOR

Let us first provide a general construction and definition for a Floquet topological insulator in a generic lattice model, and then discuss a specific realization: a HgTe/CdTe quantum well. The generic many-body Hamiltonian of interest is

$$\hat{\mathcal{H}}(t) = \sum_{\mathbf{k} \in \text{BZ}} H_{nm}(\mathbf{k}, t) \hat{c}_{n,\mathbf{k}}^\dagger \hat{c}_{m,\mathbf{k}} + \text{h. c.}, \quad (1)$$

where  $\hat{c}_{n,\mathbf{k}}^\dagger$  and  $\hat{c}_{m,\mathbf{k}}$  are fermion creation/annihilation operators,  $\mathbf{k}$  is the momentum defined in the Brillouin

zone, and the Latin indices,  $n, m = 1, 2, \dots, N$  label some internal degrees of freedom (*e.g.*, spin, sublattice, layer indices, etc.). The  $N \times N$   $\mathbf{k}$ -dependent matrix  $\tilde{H}(\mathbf{k}, t)$  is determined by lattice hoppings and/or external fields, which are periodic in time,  $\tilde{H}(T + t) = \tilde{H}(t)$ .

First, we recall that without the time-dependence, the topological classification reduces to an analysis of the matrix function,  $\tilde{H}(\mathbf{k})$ , and is determined by its spectrum. [20, 21]. An interesting question is whether a topological classification is possible in non-equilibrium, *i.e.*, when the single-particle Hamiltonian,  $\tilde{H}(\mathbf{k}, t)$ , in Eq. (1) does have an explicit time-dependence and whether there are observable physical phenomena associated with this non-trivial topology. Consider the single-particle Schrödinger equation associated with Eq. (1):

$$[\tilde{H}(\mathbf{k}, t) - i\tilde{I}\partial_t] \Psi_{\mathbf{k}}(t) = 0, \text{ with } \tilde{H}(\mathbf{k}, t) = \tilde{H}(\mathbf{k}, t + T) \quad (2)$$

The Bloch-Floquet theory states that the solutions to Eq. (2) have the form  $\Psi_{\mathbf{k}}(t) = \check{S}_{\mathbf{k}}(t)\Psi_{\mathbf{k}}(0)$ , where the unitary evolution is given by the product of a periodic unitary part and a Floquet exponential

$$\check{S}_{\mathbf{k}}(t) = \check{P}_{\mathbf{k}}(t) \exp[-i\check{H}_F(\mathbf{k})t], \text{ with } \check{P}_{\mathbf{k}}(t) = \check{P}_{\mathbf{k}}(t + T) \quad (3)$$

where  $\check{H}_F(\mathbf{k})$  is a self-adjoint *time-independent* matrix, associated with the Floquet operator  $[\tilde{H}(\mathbf{k}, t) - i\tilde{I}\partial_t]$  acting in the space of periodic functions  $\Phi(t) = \Phi(t + T)$ , where it leads to a time-independent eigenvalue problem,  $[\tilde{H}(\mathbf{k}, t) - i\tilde{I}\partial_t] \Phi(\mathbf{k}, t) = \varepsilon(\mathbf{k})\Phi(\mathbf{k}, t)$ . The quasi-energies  $\varepsilon(\mathbf{k})$  are the eigenvalues of the matrix  $\check{H}_F(\mathbf{k})$  in Eq. (3), and in the cases of interest can be divided into separate bands. The full single-particle wave-function is therefore given by  $\Psi(t) = e^{-i\varepsilon t}\Phi(t)$ . Note that the quasi-energies are defined modulo the frequency  $\omega = 2\pi/T$ .

The Floquet topological insulator is defined through the topological properties of the time-independent Floquet operator  $\check{H}_F(\mathbf{k})$ , in accordance with the existing topological classification of equilibrium Hamiltonians [20, 21]. Most importantly, we show below that the FTI is not only a mathematical concept, but it has immediate physical consequences in the form of robust edge states that appear in a finite system in the non-equilibrium regime. These hallmark boundary modes were found to be only weakly time-dependent [through the envelope function determined by the matrix  $\check{P}_{\mathbf{k}}(t)$  in Eq. 3]. Furthermore, we explicitly demonstrate within a specific model that not only topological insulator properties may survive in non-equilibrium, but they can be induced via a simple non-equilibrium perturbation in an otherwise topologically trivial system. Using the specific model describing a HgTe/CdTe quantum wells, we show that a carefully chosen non-equilibrium perturbation may be utilized to turn the topological properties on and off. We discuss various methods to realize such a perturbation using experimentally accessible electromagnetic radiation in the microwave-THz regime.

## TOPOLOGICAL TRANSITION IN HgTe/CdTe HETEROSTRUCTURES

Below we outline a proposal for the realization of a FTI in Zincblende structures such as the HgTe/CdTe heterostructure which are in the trivial phase ( $d < d_c$  in Ref. 5). Consider the Hamiltonian

$$H(k_x, k_y) = \begin{pmatrix} \tilde{H}(\mathbf{k}) & 0 \\ 0 & \tilde{H}^*(-\mathbf{k}) \end{pmatrix} \quad (4)$$

where

$$\tilde{H}(\mathbf{k}) = \epsilon(\mathbf{k})\tilde{I} + \mathbf{d}(\mathbf{k}) \cdot \tilde{\sigma}, \quad (5)$$

$\mathbf{k} = (k_x, k_y)$  is the two dimensional wave vector, and  $\tilde{\sigma} = (\tilde{\sigma}_x, \tilde{\sigma}_y, \tilde{\sigma}_z)$  are the Pauli matrices. The vector,  $\mathbf{d}(\mathbf{k})$ , is an effective spin-orbit field. Equations (4) and (5) represent the effective Hamiltonian of HgTe/CdTe heterojunctions [5]. In these systems, the upper block  $\tilde{H}(\mathbf{k})$  is spanned by states with  $m_J = (1/2, 3/2)$ , while the lower block is spanned by states with  $m_J = (-1/2, -3/2)$ . The lower block  $\tilde{H}^*(-\mathbf{k})$  is the time reversal partner of the upper block, and in the following we shall focus our attention to the upper block of Eq. (4) only.

The Hamiltonian (5) is diagonalized via a  $\mathbf{k}$ -dependent  $SU(2)$  rotation, that sets the z-axis for the pseudo-spin along the vector  $\mathbf{d}(\mathbf{k})$ . There are two double-degenerate bands with energies  $\epsilon_{\pm}(\mathbf{k}) = \epsilon(\mathbf{k}) \pm |\mathbf{d}(\mathbf{k})|$ . Within each sub-block, the TKNN formula provides the sub-band Chern number [22], which for the Hamiltonian (5) can be expressed as an integer counting the number of times the vector  $\hat{\mathbf{d}}(\mathbf{k})$  wraps around the unit sphere as  $\mathbf{k}$  wraps around the entire FBZ. In integral form, it is given by

$$C_{\pm} = \pm \frac{1}{4\pi} \int d^2\mathbf{k} \hat{\mathbf{d}}(\mathbf{k}) \cdot [\partial_{k_x} \hat{\mathbf{d}}(\mathbf{k}) \times \partial_{k_y} \hat{\mathbf{d}}(\mathbf{k})], \quad (6)$$

where  $\hat{\mathbf{d}}(\mathbf{k}) = \mathbf{d}(\mathbf{k})/|\mathbf{d}(\mathbf{k})|$  is a unit vector and the  $(\pm)$  indices label the two bands.

This elegant mathematical construction yields also important physical consequences, as it is related to the quantized Hall conductance associated with an energy band,

$$\sigma_{xy} = \frac{e^2}{h} C. \quad (7)$$

Around the  $\Gamma$  point of the first Brillouin zone (FBZ) we can expand the vector  $\mathbf{d}(\mathbf{k})$  as [5, 23]

$$\mathbf{d}(\mathbf{k}) = (Ak_x, Ak_y, M - Bk^2) \quad (8)$$

where the parameters  $A < 0$ ,  $B > 0$  and  $M$  depend on the thickness of the quantum well and on parameters of the materials. We can easily see that the Chern number implied by  $\mathbf{d}(\mathbf{k})$  depends crucially on the relative sign

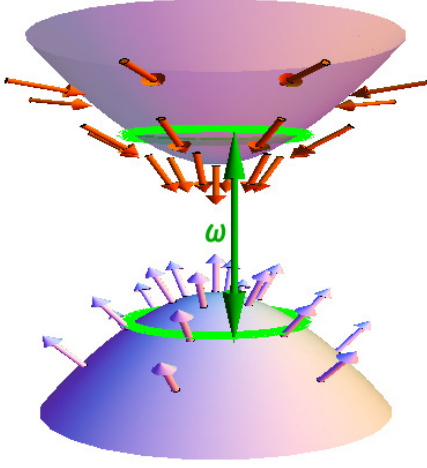


FIG. 1. Energy dispersion  $\epsilon(\mathbf{k})$  and pseudospin configuration  $-\hat{\mathbf{d}}(\mathbf{k})$  for the original bands of  $\tilde{H}(\mathbf{k})$  in the non topological phase ( $M/B < 0$ ). The non-topological phase is characterized by a spin-texture which does not wrap around the unit sphere. Upon application of a periodic modulation of frequency  $\omega$  bigger than the band gap, a resonance appears; the green circles and arrow depict the resonance condition.

of  $M$  and  $B$ . Within the approximation of Eq. (8), far away from the  $\Gamma$  point,  $\mathbf{d}(\mathbf{k})$  must point south (in the negative  $z$  direction). At the  $\Gamma$  point,  $\mathbf{d}(\mathbf{k})$  is pointing north for  $M > 0$ , but south for  $M < 0$ . For the simplified band structure, the Chern numbers are clearly  $C_{\pm} = \pm [1 + \text{sign}(M/B)]/2$ . For a generic band structure corresponding to Eq. (8) near the  $\Gamma$ -point, the same logic applies, and we can easily see that a change of sign in  $M$  induces a change of the Chern number,  $C$ , by 1.

We now show that a similar non-trivial topological structure can be induced in such quantum wells, starting with the non-topological phase, via periodic modulation of the Hamiltonian, which allows transitions between same-momentum states with energy difference of  $\hbar\omega$ . This creates a circle in the FBZ where transitions between the valence and conduction band are at resonance (see Fig. 1). We intend to use the modulation to reshuffle the spectrum such that the resulting valence band consists of two parts: the original valence band outside the resonance circle drawn in Fig. 1, and the original conduction band inside the resonance circle, near the  $\Gamma$  point. From Fig. 1, we see that this indeed leads to the desired structure, with the reshuffled pseudospin configuration pointing south near the  $\Gamma$  point and north at large  $k$ -values (for  $M < 0$ ). On the resonance circle, we expect an avoided crossing separating the reshuffled lower band from the upper band.

## FLOQUET TOPOLOGICAL INSULATOR IN A NON-EQUILIBRIUM $(Cd, Hg)Te$ HETEROSTRUCTURE

Let us next consider the Floquet problem in a Zincblende spectrum in detail. We add a time dependent field to the Hamiltonian (5)

$$\tilde{V}(t) = \mathbf{V} \cdot \hat{\boldsymbol{\sigma}} \cos(\omega t) \quad (9)$$

where  $\mathbf{V}$  is a three-dimensional vector, which has to be carefully chosen to obtain the desired result. It is convenient to transform the bare Hamiltonian to a “rotating frame of reference” such that the bottom band is shifted by  $\hbar\omega$ . This is achieved using the unitary transformation  $\tilde{U}(\mathbf{k}, t) = \tilde{P}_+(\mathbf{k}) + \tilde{P}_-(\mathbf{k})e^{i\omega t}$ , where  $\tilde{P}_{\pm}(\mathbf{k}) = \frac{1}{2} [I \pm \hat{\mathbf{d}}(\mathbf{k}) \cdot \hat{\boldsymbol{\sigma}}]$  are projectors on the of upper and lower bands of  $H(\mathbf{k})$ . This results in the following Hamiltonian:

$$\tilde{H}_I(t) = \tilde{P}_+(\mathbf{k})\epsilon_+(\mathbf{k}) + \tilde{P}_-(\mathbf{k})[\epsilon_-(\mathbf{k}) + \omega] + \tilde{U}\tilde{V}(t)\tilde{U}^\dagger \quad (10)$$

where  $\epsilon_{\pm}(\mathbf{k})$  are the energies corresponding to  $\tilde{P}_{\pm}(\mathbf{k})$ . In the “rotating” picture, the two bands cross if  $\omega$  is larger than the gap  $M$ . The second term in the right-hand-side of Eq. (10) is the driving term, which directly couples the bands and has a time-independent component.

The solution of  $H_I$  can also be given in terms of a spinor pointing along a unit vector,  $\hat{\mathbf{n}}_{\mathbf{k}}$ , which will play the same role as  $\hat{\mathbf{d}}(\mathbf{k})$  for the stationary  $\tilde{H}(\mathbf{k})$ .  $\hat{\mathbf{n}}_{\mathbf{k}}$  will encode the topological properties of the FTI.

$H_I$  is solved by the eigenstates  $|\psi_I^{\pm}(\mathbf{k})\rangle$ , which for the values of momenta,  $\mathbf{k}$ , away from the resonance ring are only weakly modified compared to the equilibrium,  $V = 0$ , case. We define the vector  $\hat{\mathbf{n}}_{\mathbf{k}} = \langle \psi_I^-(\mathbf{k}) | \hat{\boldsymbol{\sigma}} | \psi_I^-(\mathbf{k}) \rangle$ , which characterizes the pseudospin configuration in the lower ( $-$ ) band of  $H_I$ . The vector  $\hat{\mathbf{n}}_{\mathbf{k}}$  is plotted in Fig. 2 for  $M/B < 0$ . Indeed, near the  $\Gamma$  point we see that  $\hat{\mathbf{n}}_{\mathbf{k}}$  points towards the south pole, and for larger values of  $\mathbf{k}$ , the band consists of the original lower band, and therefore  $\hat{\mathbf{n}}_{\mathbf{k}}$  points towards the northern hemisphere for these  $\mathbf{k}$  values. These two regimes are separated by the resonance ring, denoted by  $\gamma$ , for which  $\omega = e^+(\mathbf{k}) - e^-(\mathbf{k})$  (the green curve in Fig. 1).

The topological aspects of the reshuffled lower band depends crucially on the properties of  $\hat{\mathbf{n}}_{\mathbf{k}}$  on  $\gamma$ , which are, in turn, inherited from the geometric properties of the driving potential, encoded in  $\mathbf{V}$ . These are best illustrated by employing the rotating wave approximation, as we shall proceed to do below. An exact numerical solution will be presented in the next section.

The driving field  $\tilde{V}(t)$  contains both counter-rotating and co-rotating terms. In the rotating wave approximation it is given by

$$\tilde{V}_{\text{RWA}} = \tilde{P}_+(\mathbf{k})(\mathbf{V} \cdot \hat{\boldsymbol{\sigma}})\tilde{P}_-(\mathbf{k}) + \tilde{P}_-(\mathbf{k})(\mathbf{V} \cdot \hat{\boldsymbol{\sigma}})\tilde{P}_+(\mathbf{k}) \quad (11)$$

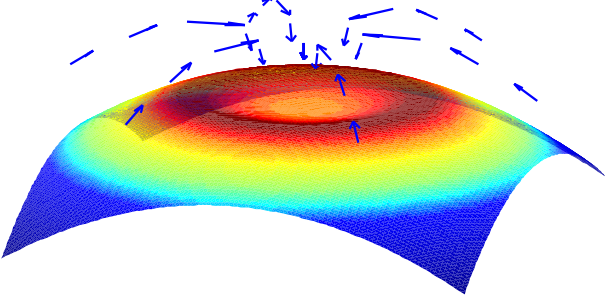


FIG. 2. Pseudospin configuration  $\hat{\mathbf{n}}_{\mathbf{k}}$  (blue arrows) and dispersion of the lower band of  $H_I$ . Note the dip in the energy surface near  $\mathbf{k} = 0$ , resulting from the reshuffling of the lower and upper bands of  $\tilde{H}(\mathbf{k})$ .

Next, we decompose the vector  $\mathbf{V}$  as follows

$$\mathbf{V} = (\mathbf{V} \cdot \hat{\mathbf{d}}(\mathbf{k})) \hat{\mathbf{d}}(\mathbf{k}) + \mathbf{V}_{\perp}(\mathbf{k}). \quad (12)$$

A substitution in Eq. (11) gives

$$\tilde{V}_{\text{RWA}} = \mathbf{V}_{\perp} \cdot \tilde{\boldsymbol{\sigma}}. \quad (13)$$

On the curve  $\gamma$  we have:

$$\hat{\mathbf{n}}_{\mathbf{k}} = -\mathbf{V}_{\perp}(\mathbf{k})/|\mathbf{V}_{\perp}(\mathbf{k})|. \quad (14)$$

We can define a topological invariant  $C^F$  similar to  $C$  in Eq. (6), by replacing  $\hat{\mathbf{d}}(\mathbf{k})$  with  $\hat{\mathbf{n}}_{\mathbf{k}}$ . In order for  $\hat{\mathbf{n}}_{\mathbf{k}}$  to have a non-vanishing  $C^F$ , it needs to wrap around the unit sphere. A necessary condition is that on the curve  $\gamma$ , it forms a loop that winds around the north pole. Now,  $\mathbf{V}_{\perp}(\mathbf{k})$  lies on the plane defined by  $\hat{\mathbf{d}}(\mathbf{k})$  and  $\mathbf{V}$ . For the values of  $\mathbf{k}$  which are on-resonance,  $\hat{\mathbf{d}}(\mathbf{k})$  traces a closed loop on the unit sphere which encircles the north pole. Therefore, if the driving field vector  $\mathbf{V}$  points to a point on the Bloch sphere which is encircled by this loop,  $\mathbf{V}_{\perp}(\mathbf{k})$  will also trace (a different) loop on the sphere which encircles the north pole, as illustrated by Fig. 3.

Under the conditions stated above and with  $M < 0$ , the vector field  $\hat{\mathbf{n}}_{\mathbf{k}}$  starts from the south pole at  $\Gamma$  point and continues smoothly to the northern hemisphere for larger values of  $|\mathbf{k}|$  while winding around the equator. For values of  $\mathbf{k}$  further away from the curve  $\gamma$ ,  $\hat{\mathbf{n}}_{\mathbf{k}} \approx -\hat{\mathbf{d}}(\mathbf{k})$  as the driving field is off resonance there. The contribution of these  $\mathbf{k}$ 's to  $C^F$  is therefore equal to their contribution to  $C$ . Therefore it is evident that  $C^F = C + 1$ . Note that for  $M > 0$ ,  $C^F = C - 1$ .

A comment is in order regarding the time dependence of  $C^F$ . Since the solutions to the time dependent Schrödinger equation are given by transforming back to the Schrödinger picture,

$$|\psi^{\pm}(t, \mathbf{k})\rangle = U(t)|\psi_I^{\pm}(\mathbf{k})\rangle, \quad (15)$$

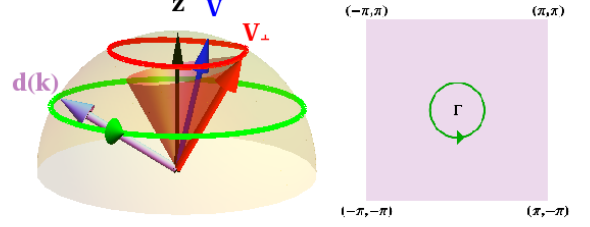


FIG. 3. The geometrical condition for creating topological quasi-energy bands. The green arrow and circle depicts  $\hat{\mathbf{d}}(\mathbf{k})$  on the curve  $\gamma$  in the FBZ for which the resonant condition holds. The red arrow and cone depicts  $\mathbf{V}_{\perp}(\mathbf{k})$  on  $\gamma$ . The blue arrow depicts the driving field vector  $\mathbf{V}$ . As long as  $\mathbf{V}$  points within the loop traced by  $\hat{\mathbf{d}}(\mathbf{k})$ , the vector  $\mathbf{V}_{\perp}(\mathbf{k})$  winds around the north pole, which is indicated by the black arrow.

the pseudospin configuration in the Brillouin zone of these solutions ,

$$\hat{\mathbf{n}}_{\mathbf{k}}(t) = \langle \psi^{-}(\mathbf{k}, t) | \tilde{\boldsymbol{\sigma}} | \psi^{-}(\mathbf{k}, t) \rangle, \quad (16)$$

will also depend on time. As long as  $H_I$  is non-degenerate in the FBZ, which implies that  $\hat{\mathbf{n}}_{\mathbf{k}}(t)$  is well defined,  $C^F$  will be quantized to an integer. As for  $C$ , also  $C^F$  is a topological invariant which is robust to smooth changes in  $\hat{\mathbf{n}}_{\mathbf{k}}(t)$  which are not singular at any point in the FBZ. Therefore,  $C^F$  *does not* depend on time, although the pseudospin configurations  $\hat{\mathbf{n}}_{\mathbf{k}}(t)$  do, and we can calculate  $C^F$  using  $\hat{\mathbf{n}}_{\mathbf{k}}$ .

## NON-EQUILIBRIUM EDGE STATES

One of the most striking results of the above considerations is the existence of helical edge states once the time dependent field is turned on. Below we demonstrate the formation of edge states in a tight binding model which contains the essential features of Eq. (5). The Fourier transform of the spin-orbit coupling vector,  $\mathbf{d}(\mathbf{k})$  in the corresponding lattice model is given by, c.f., Eq. (8),

$$\mathbf{d}(\mathbf{k}) = (A \sin k_x, A \sin k_y, M - 4B + 2B[\cos k_x + \cos k_y]). \quad (17)$$

We consider the above model with the time dependent field of the form  $V_0 \sigma_z \cos(\omega t)$  in the strip geometry, with periodic boundary condition in the  $x$  direction, and vanishing boundary conditions at  $y = 0, L$ .

We solve the Floquet equation numerically by moving to frequency space and truncating number of harmonics. The wave vector  $k_x$  is therefore a good quantum number, and the solutions  $\Phi(t)$  are characterized by  $\varepsilon$  and  $k_x$ . The quasi-energies for this geometry is displayed in Fig. 4.

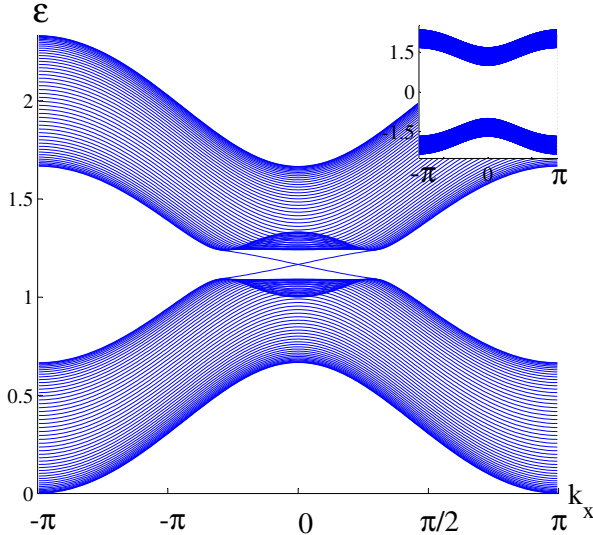


FIG. 4. Quasi-energy spectrum of the Floquet equation (3) of the Hamiltonian (17), in the strip geometry: periodic boundary conditions in the  $x$  direction, and vanishing ones in the  $y$  direction. The driving field was taken to be  $\mathbf{V} = \hat{\mathbf{z}}$  direction. The horizontal axis labels the momentum  $k_x$ . The vertical axis labels the quasi-energies in units of  $|M|$ . Two linearly dispersing chiral edge modes traverse the gap in the quasi-energy spectrum. The parameters used are  $\omega = 2.3|M|$ ,  $|\mathbf{V}| = A = |B| = 0.2|M|$ . The inset shows the dispersion of the original Hamiltonian (17), for the same parameters.

The quasi-energies of the bottom and top band represent modes which are extended spatially, while for each value of  $k_x$  there are two modes which are localized in the  $y$  direction.

As is evident from Fig. 4, the *quasi-energies* of these modes disperse linearly,  $\varepsilon(k_x) \propto k_x$ , hence they are propagating with a fixed velocity. Consider a wave packet which is initially described by  $f_0(k_x)$ . From equation (3) we see that it will evolve into  $\psi(t) = \int dk_x e^{i\varepsilon(k_x)t} f_0(k_x) \Phi_{k_x}^e(y, t)$ , where  $\Phi_{k_x}^e$  denotes the quasi energy *edge* states with momentum  $k_x$ . Clearly, this will give a velocity of  $\langle \dot{x} \rangle = \int dk_x |f(k_x)|^2 \frac{\partial \varepsilon}{\partial k_x}$ .

In general, the solutions  $\Phi_{\varepsilon, k_x}(t)$  are time-dependent. An important finding is that the density edge modes are only very weakly dependent on time. This can be seen in Fig. 5, in which we plot the time dependence of the density profile of these modes.

## EXPERIMENTAL REALIZATION OF THE FTI

To experimentally realize the proposed state, we need identify a proper time-dependent interaction in the HgTe/CdTe wells. Below we consider several options, of which the most promising one uses a periodic electric

field, and the strong linear Stark effect that arises due to the unique band structure.

First, we note that when considering the realization of the above ideas in HgTe/CdTe quantum wells, one needs to consider the full Hamiltonian (4). As can be seen by inspecting Eq. (12), for a simple driving field of the form Eq.(9) with  $\mathbf{k}$ -independent  $\mathbf{V}$ , the Chern numbers  $C^F$  of each block depends only on the winding of the vector  $\hat{\mathbf{d}}(\mathbf{k})$ . Therefore, the two blocks will exhibit opposite  $C^F$ , resulting in two *counter*-propagating helical edge modes. For time independent Hamiltonians, such a state is only topologically distinct from a trivial state when  $\mathcal{T}H\mathcal{T}^{-1} = H$  where  $\mathcal{T}$  is the anti-unitary time reversal operator satisfying  $\mathcal{T}^2 = -1$ . Similarly, in the time-periodic case, the same restriction on the Hamiltonian in the rotating wave approximation leads to robustness of the counter propagating edge states. To obey this condition, a perturbation of the form (9) leading to  $\mathbf{V}_\perp^U$  in the upper block needs to be accompanied by  $\mathbf{V}_\perp^L = (-V_{\perp x}^U, V_{\perp y}^U, V_{\perp z}^U)$  in the lower block. On the other hand, the electric field realization is an example of a *k-dependent* perturbation which allows for two *co*-propagating edge modes.

*Magnetic field realization* – Perhaps the simplest realization of a time dependent perturbation of the form (9) is by a microwave-THz oscillating magnetic field, polarized in the  $\mathbf{z}$  direction. The effect of Zeeman energies in thin Hg/CdTe quantum wells can be evaluated by recalling that the effective model (4) includes states with  $m_J = \pm(1/2, 3/2)$  in the upper and lower block respectively. This would result in an effective Zeeman splitting between the two states in each block [23]. The value for the g-factor for HgTe semiconductor quantum wells was measured to be  $g \approx 20$  [24]. Therefore, a gap in the quasienergy spectrum on the order of 0.1K can be achieved using magnetic fields of 10mT. Bigger gaps may be achieved by using Se instead of Te, as its g-factor is roughly twice as large [25].

The time dependent magnetic field will lead to  $\check{V}(t)$  with *opposite signs* for the upper and lower blocks, and hence does not obey the condition discussed at the beginning of this section. Therefore, the edge modes can have an anti-crossing at their intersection point. Nevertheless, the matrix elements that couple the edge modes may be strongly suppressed. These stem from (i)  $H_Z$  itself, which is only possible due mixing of  $m_J = \pm 1/2$  with  $m_J = \mp 3/2$  states [26], and is therefore expected to be much smaller than the gap in the quasi-energy spectrum deep in the  $M < 0$  phase, and (ii) Coupling of the magnetic field to orbital circulations of the modes, whose magnitude can be estimated as  $e \frac{\partial \varepsilon}{\partial k} \xi B$ , where  $\xi$  is the extent of the edge modes [6]. This can be rewritten as  $(g\mu_B B)^2/E_0$  with  $E_0 = \frac{q\hbar^2 k_0 \xi^{-1}}{m_e}$ , with  $k_0$  the momentum where the edge modes join the bulk. With fields on the order of 10mT, we have  $E_0 \gg g\mu_B B$  giving a small



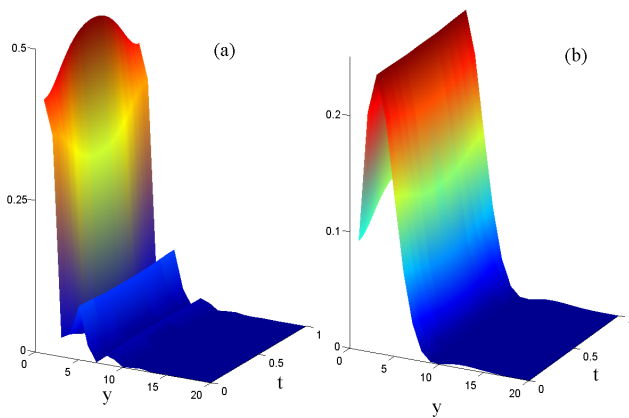


FIG. 5. Density of edge mode as function of time,  $|\phi(y, t)|^2$ , (a) for  $k_x = 0$ , and (b) for  $k_x = 0.84$ , where the edge modes meet the bulk states. The horizontal axis display the distance from the edge,  $y$ , in units of the lattice constant, and the time in units of  $2\pi/\omega$ . Only the density for the 20 lattice sites closest to the edge are shown for clarity.

coupling compared to the gap.

*Stress Modulation* – An experimental realization that can potentially lead to a perturbation  $\hat{V}(t)$  that effectively respects time reversal invariance is a stress modulation of the quantum wells using piezo-electric materials, which would lead to modulation of the parameter  $m$  in (5).

*Electric field realization* – An in-plane electric field is perhaps the most promising route to the FTI, can produce large gaps in the quasi-energy spectrum (compared the Zeeman case), and leads to robust edge states. The electric field is given by

$$\vec{E} = \text{Re}(\mathcal{E} \cdot \exp i\omega t) i \nabla_{\mathbf{k}}. \quad (18)$$

Inserting this into Eq. (11), we get

$$\mathbf{V}_{\perp}(\mathbf{k}) = \hat{\mathbf{d}}(\mathbf{k}) \times (\text{Re}\mathcal{E} \cdot \nabla_{\mathbf{k}}) \hat{\mathbf{d}}(\mathbf{k}) - (\text{Im}\mathcal{E} \cdot \nabla_{\mathbf{k}}) \hat{\mathbf{d}}(\mathbf{k}). \quad (19)$$

As before, the vector field  $\mathbf{V}_{\perp}(\mathbf{k})$  is orthogonal to  $\hat{\mathbf{d}}(\mathbf{k})$ , and again, we would like it to wind around the north pole. Now if we take  $\mathcal{E} = \mathcal{E}(-i\hat{\mathbf{x}} + \hat{\mathbf{y}})$  we get, expanding Eq.(19) to second order in  $k_x, k_y$ ,

$$\mathbf{V}_{\perp}(\mathbf{k}) = \frac{A(A^2 - 4BM)\mathcal{E}}{M^3} \left[ \frac{1}{2}(k_x^2 - k_y^2)\hat{\mathbf{x}} + k_x k_y \hat{\mathbf{y}} \right]. \quad (20)$$

Evidently, the vector field  $\mathbf{V}_{\perp}(\mathbf{k})$  winds twice around the equator. Therefore, for the above choice of  $\mathcal{E}$ , the Chern numbers will be  $C^F = \pm 2$ . We note that for the lower block will have  $C^F = 0$ . Therefore, each edge of the system will have two *co*-propagating chiral modes, with spin which in the sector of  $m_J = 1/2, 3/2$ . Naturally, a choice of  $\mathcal{E} = \mathcal{E}(i\hat{\mathbf{x}} + \hat{\mathbf{y}})$  will give  $C^F = \pm 2$  for the lower block and  $C^F = 0$  for the upper block. The evolution with the oscillating electric field is topologically distinct from the trivial one, as can be seen by the fact that the two

*co*-propagating edge modes cannot become gapped. For HgTe/CdTe quantum wells with thickness of  $58\text{\AA}$ [5], we have  $|\mathbf{V}(\mathbf{k})/\mathcal{E}| \approx 1\text{mm}$ , which leads to a gap in the quasi-energy spectrum on the order of  $10K$  already for modest electric fields on the order of  $1\frac{\text{V}}{\text{m}}$  which are achievable with powers  $< 1\text{mW}$ . We note that decreasing the well thickness increases [27] the value of  $|A/M|$ , which can help achieve even larger gaps in the quasi energy spectrum.

## CONCLUSIONS

In conclusion, we showed that the quasi-energy spectrum of an otherwise ordinary band insulator irradiated by electromagnetic fields can exhibit non-trivial topological quantum numbers and chiral edge modes. A realization of this ideas in Zincblende systems, such as HgTe/CdTe semiconducting quantum wells, can lead to topological insulators in two symmetry classes of evolutions (the analogs of classes A and AII in [20]), with either *co*- or counter-propagating helical edge modes.

An important question that we did not touch upon is the non-equilibrium onset and steady states [28] of the driven systems. We emphasize that in the presence of the time dependent fields, response functions including Hall conductivity will be determined not only by the spectrum of the Floquet operator, but also by the distribution of electrons on this spectrum. These in turn depend on the specific relaxation mechanisms present in the system, such as electron-phonon mechanisms which we expect to be dominant in solid state systems [29, 30]. An interesting observation here is that the average energies of the edge modes lie in the original bandgap.

One way to minimize the unwanted non-equilibrium heating effects would be to use an adiabatic build-up of the Floquet topological insulator state, e.g. with the frequency of the modulation gradually increasing from zero. This should result, at least initially, in a filled lower Floquet band. Nevertheless, the scattering events will lead to a relaxation from the conduction band into the valence band of the original system and will always play role by producing mobile bulk quasiparticles. Perhaps this relaxation could be suppressed by restricting the corresponding optical modes in the environment. An analysis of the non-equilibrium states of the system will be the subject of future work.

We thank Joseph Avron, Assa Auerbach, Andrei Bernevig, James Eisenstein, Lukasz Fidkowski, Victor Gurarie, Israel Klich, and Anatoli Polkovnikov for illuminating conversations. This research was supported by DARPA (GR, VG), NSF grants PHY-0456720 and PHY-0803371 (GR, NL). NL acknowledges the financial support of the Rothschild Foundation and the Gordon and Betty Moore Foundation.

- 
- [1] Liang Fu, and C. L. Kane, Phys. Rev. Lett. **100**, 096407 (2008).
  - [2] G. Moore and N. Read, Nucl. Phys. B **360**, 362 (1991).
  - [3] I. Žutić, J. Fabian, and S. Das Sarma, Rev. Mod. Phys. **76**, 323 (2004).
  - [4] C. Nayak, S. H. Simon, A. Stern, M. Freedman, and S. Das Sarma, Rev. Mod. Phys. **80**, 1083 (2008).
  - [5] B. A. Bernevig, T. L. Hughes, and S-C. Zhang, Science **314**, 1757 (2006).
  - [6] M. Knig, S. Wiedmann, C. Brne, A. Roth, H. Buhmann, L. W. Molenkamp, X-L. Qi, and S-C. Zhang, Science **318**, 766 (2007).
  - [7] D. Hsieh, D. Qian, L. Wray, Y. Xia, Y. S. Hor, R. J. Cava and M. Z. Hasan, Nature **452**, 970 (2008).
  - [8] Y. Xia, D. Qian, D. Hsieh, L. Wray, A. Pal, H. Lin, A. Bansil, D. Grauer, Y. S. Hor, R. J. Cava and M. Z. Hasan, Nature Physics **5**, 398 (2009).
  - [9] H. Zhang, C-X. Liu, X-L. Qi, X. Dai, Z. Fang, and S-C. Zhang, Nature Physics **5**, 438, (2009).
  - [10] T. Kitagawa, M. S. Rudner, E. Berg, and E. Demler, arXiv:1003.1729.
  - [11] A. S. Sørensen, E. Demler, and M. D. Lukin, Phys. Rev. Lett. **94** 086803 (2005).
  - [12] T. D. Stanescu, V. Galitski, J. Y. Vaishnav, C. W. Clark, and S. Das Sarma, Phys. Rev. A **79**, 053639 (2009).
  - [13] T. Oka and H. Aoki, Phys. Rev. B **79**, 081406(R) (2009).
  - [14] R. G. Mani, J. H. Smet, K. von Klitzing, V. Narayana-murti, W. B. Johnson, and V. Umansky, Nature **420**, 646 (2002).
  - [15] M. A. Zudov and R. R. Du, L. N. Pfeiffer and K. W. West, Phys. Rev. Lett. **90**, 046807 (2003).
  - [16] A. Auerbach and G. V. Pai, Phys. Rev. B **76**, 205318 (2007).
  - [17] I. A. Dmitriev, M. G. Vavilov, I. L. Aleiner, A. D. Mirlin, and D. G. Polyakov, Phys. Rev. B **71**, 115316 (2005).
  - [18] J. Inoue and A. Tanaka, arXiv:1006.5283.
  - [19] F. D. M. Haldane, Phys. Rev. Lett. **61**, 2015 (1988).
  - [20] A. P. Schnyder, S. Ryu, A. Furusaki, and A. W. Ludwig, Phys. Rev. B **78**, 195125 (2008).
  - [21] A. Kitaev, AIP Conf. Proc. **1134**, 22 (2009), arXiv: 0901.2686.
  - [22] D. J. Thouless, M. Kohmoto, P. Nightingale and M. den Nijs, Phys. Rev. Lett. **49**, 405 (1982).
  - [23] E. G. Novik, A. P. Pfeuffer-Jeschke, T. Jungwirth, V. Latussek, C. R. Becker, G. Landwehr, H. Buhmann, and L. W. Molenkamp, Phys. Rev. B **72**, 035321 (2005).
  - [24] X. C. Zhang, K. Ortner, A. Pfeuffer-Jeschke, C. R. Becker, and G. Landwehr, Phys. Rev. B **69** 115340, (2004).
  - [25] M. Willatzen, M. Cardona, and N. E. Christensen, Phys. Rev. B. **51**, 17992 (1995).
  - [26] X. Dai, T. L. Hughes, X-L. Qi, Z. Fang and S-C Zhang, Phys. Rev. B. **77**, 125319 (2008).
  - [27] D. G. Rothe, R. W. Reinthaler, C-X Liu, L. W. Molenkamp, S-C. Zhang and E. M. Hankiewicz, New J. Phys. **12**, 065012 (2010).
  - [28] A. Robertson and V. M. Galitski, Phys. Rev. A **80**, 063609 (2009).
  - [29] G. M. Eliashberg, Pis'ma Zh. Eksp. Teor. Fiz. **11**, 186 (1970); JETP Lett. **11**, 114 (1970).
  - [30] G. M. Eliashberg, in "Nonequilibrium Superconductivity," edited by D. N. Langenberg and A. I. Larkin (North-Holland, New York, 1986).